Appl. Phys. B 65, 499–503 (1997)

Applied Physics B Lasers and Optics

Index of refraction, optical activity and electro-optic coefficient of bismuth titanium oxide ($Bi_{12}TiO_{20}$)

D.G. Papazoglou, A.G. Apostolidis, E.D. Vanidhis

Aristotle University of Thessaloniki, Department of Physics-Solid State, Section 313-1, 540 06 Thessaloniki, Greece
(Fax: +30-31/998019, E-mail: optlab@ccf.auth.gr)

Received: 22 December 1996/Revised version: 21 March 1997

Abstract. The index of refraction, optical activity, and linear electro-optic coefficient are basic optical parameters determining the photorefractive behaviour of $Bi_{12}TiO_{20}$. The first two can be measured by simple and classical methods, but the coexistence of optical activity, electrogyration, field-induced linear birefringence, and piezoelectric and photoelastic effects in photorefractive materials such as $Bi_{12}TiO_{20}$ complicate the measurement of the electro-optic coefficient. For normal incidence of linearly polarized light we derive analytic expressions for the polarization of light that has passed through the crystal. The ellipticity of the polarization is a function of the electric-field-induced linear birefringence and hence of the electro-optic coefficient of the crystal. Therefore measurement of the ellipticity as a function of an electric field externally applied to the crystal leads to an electro-optic coefficient r_{41} of 5.3 ± 0.1 pm/V.

PACS: 42.65

Electro-optic photoconducting crystals of the sillenite type [$Bi_{12}GeO_{20}$ (BGO), $Bi_{12}TiO_{20}$ (BTO), $Bi_{12}SiO_{20}$ (BSO)] are currently widely used as image-recording media for real-time holographic interferometry and spatial light modulation, for example [1–3]. BTO is a cubic crystal, belonging to the point-group 23. It exhibits optical activity and electrogyration and is linearly birefringent when an electric field is present. Although there is sufficient published data of the optical parameters of BGO and BSO [4–10], there is a lack of published data for BTO crystals. In particular, the index of refraction, the optical activity, and the linear electrooptic coefficient of BTO crystals are not well known.

The index of refraction and the optical activity can be measured by using conventional methods. In BTO the electro-optic tensor has three equal nonzero elements: r_{41}, r_{52} and r_{63}. The electro-optic coefficient r_{41} is an important parameter for applications with BTO, because it is linearly related to the photorefractive sensitivity. The coexistence of optical activity, electrogyration, field-induced linear birefringence, and piezoelectric and photoelastic effects make the measurement of the electro-optic coefficient quite complex.

The ellipticity of a light beam emerging from these crystals is a function of all effects mentioned above and an effective electro-optic coefficient r_{eff} is introduced. Analytic expressions are derived for the ellipticity of the light beam emerging from the crystal as a function of the crystal characteristics and of the orientation Θ_o of the polarization of the incident light beam. Measurement of the voltage at which the ellipticity becomes zero yields the effective electro-optic coefficient r_{eff}.

1 Fundamentals

1.1 Sellmeier formula for the index of refraction

For the description of the dependence of the refractive index n on the light wavelength λ we use the single-term Sellmeier relation [11]:

$$n^2(\lambda) - 1 = \frac{S_o \lambda_o^2}{1 - (\lambda_o/\lambda)^2}, \tag{1}$$

where λ_o is the average oscillator position and S_o is the average oscillator strength. The parameters S_o, λ_o in (1) can be obtained experimentally by plotting $1/(n^2-1)$ against $1/\lambda^2$. The slope of the resulting straight line gives $1/S_o$, and the infinite-wavelength intercept gives $1/(S_o\lambda_o^2)$.

1.2 Transverse configuration

The transverse configuration is most commonly used. The light beam, as shown in Fig. 1, is incident on the xz face of the crystal, which is a $(1\bar{1}0)$ plane, and propagates along the y axis. The z axis is parallel to the $\langle 001 \rangle$ axis. The electric field is applied in an orthogonal direction normal to the yz face (110). The principal crystallographic axes are denoted by x_1, x_2 and x_3, where x_3 is parallel to the z axis, and x_1 and x_2, lie in the xy plane and are oriented at 45° with respect to the x and y axes.

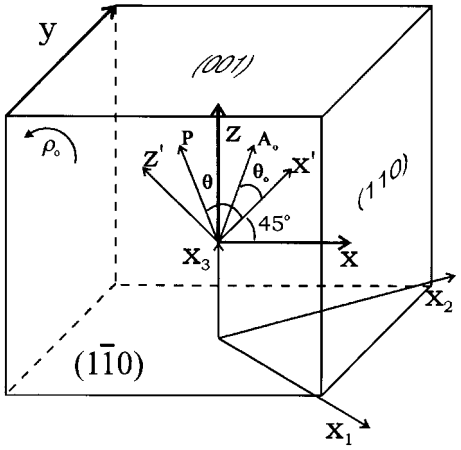

Fig. 1. Crystallographic orientation of BTO. External electric fields are applied parallel to the ⟨110⟩ axis and x' and z' are the axes of the electro-optically induced linear birefringence. The light propagates normally to the xz face. A_o is the input polarization and P shows the orientation of an analyzer behind the crystal

Light waves in cubic BTO are generally affected by the coexistence of optical activity, field-induced linear birefringence, electrogyration, and piezoelectric and photoelastic effects. The perturbation of the impermeability tensor B_{ij} due to the influence of field-induced birefringence is given by [12]

$$\Delta B_{ij}^{\mathrm{eo}} = \begin{pmatrix} 0 & 0 & \frac{\sqrt{2}}{2} r_{41} E_{\mathrm{o}} \\ 0 & 0 & \frac{\sqrt{2}}{2} r_{41} E_{\mathrm{o}} \\ \frac{\sqrt{2}}{2} r_{41} E_{\mathrm{o}} & \frac{\sqrt{2}}{2} r_{41} E_{\mathrm{o}} & 0 \end{pmatrix}, \tag{2}$$

where E_{o} is the applied field along the ⟨110⟩ axis and r_{41} is the electro-optic coefficient. On the other hand, electrogyration produces an equivalent perturbation in the gyration tensor [13]. However, because of the crystal symmetry, the electrogyratory effect vanishes in the transverse configuration [5].

In order to calculate the influence of the so-called secondary electro-optic effect (combination of inverse piezoelectric and photoelastic effects) we assume that the applied voltage results in a uniform internal field and also that the strain and stress are uniform. If the crystal is totally unclamped (stress is zero) the perturbation of the real part of the impermeability tensor is given by [12]

$$\Delta B_{ij}^{\mathrm{ph}} = \begin{pmatrix} 0 & 0 & \frac{\sqrt{2}}{2} p_{44} d_{14} E_{\mathrm{o}} \\ 0 & 0 & \frac{\sqrt{2}}{2} p_{44} d_{14} E_{\mathrm{o}} \\ \frac{\sqrt{2}}{2} p_{44} d_{14} E_{\mathrm{o}} & \frac{\sqrt{2}}{2} p_{44} d_{14} E_{\mathrm{o}} & 0 \end{pmatrix}, \tag{3}$$

where d_{14} and p_{44} are the corresponding piezoelectric and photoelastic coefficients, respectively. The total field-induced perturbation of the impermeability tensor is given by the sum of (2) and (3):

$$\Delta B_{ij}^{\mathrm{tot}} = \Delta B_{ij}^{\mathrm{eo}} + \Delta B_{ij}^{\mathrm{ph}} = \begin{pmatrix} 0 & 0 & \Gamma \\ 0 & 0 & \Gamma \\ \Gamma & \Gamma & 0 \end{pmatrix}, \tag{4}$$

where

$$\Gamma = \frac{\sqrt{2}}{2} (r_{41} + p_{44} d_{14}) E_{\mathrm{o}} .$$

As is clearly seen, it is not possible to separate the two effects (this holds for every configuration used). In any experiment with static electric fields we measure the effective electro-optic coefficient $r_{\mathrm{eff}} = r_{41} + p_{44} d_{14}$. For BTO the additional $p_{44} d_{14}$ coefficient is estimated to be of the order of 0.21 pm/V [14].

Neglecting the optical activity the above perturbations produces a linear birefringence $n \pm \Delta n$ given by the equation:

$$\Delta n = \frac{1}{2} n^3 r_{\mathrm{eff}} E_{\mathrm{o}} , \tag{5}$$

where n is the refractive index of the unperturbed crystal. The fast axis x' and the slow axis z' are oriented at 45° with respect to the x and z axes, respectively (Fig. 1).

1.3 Propagation of light in a BTO crystal

The coexistence of optical activity and field-induced birefringence means that the optical eigenwaves are elliptically polarized plane waves. The two eigenwaves have polarizations with the same ellipticity, but with opposite senses of rotation. Their major axes, which are orthogonal to each other, coincide with the principal vibration directions that would exist for this wave normal if the crystal were not optically active [12].

The phase difference ϕ, between the two eigenwaves per crystal thickness is [12]

$$\phi^2 = (2\varrho_{\mathrm{o}})^2 + \delta^2 , \tag{6}$$

where ϱ_{o} is the rotatory power and $2\varrho_{\mathrm{o}}$ and δ are the phase differences per unit crystal thickness owing to optical activity and linear birefringence, respectively. Here δ is given by

$$\delta = 2k_{\mathrm{o}} \Delta n = \frac{2\pi}{\lambda_{\mathrm{o}}} r_{\mathrm{eff}} n^3 E_{\mathrm{o}} , \tag{7}$$

where k_{o} is the vacuum wavenumber of the light beam and λ_{o} is the vacuum light wavelength. The ellipticity K (ratio of the minor to the major axis of the polarization ellipse) of the eigenwave is given by $K = \tan(\gamma/2)$ where $\tan(\gamma) = 2\varrho_{\mathrm{o}}/\delta$.

Consider now a linearly polarized light beam of amplitude A_{o} and angular frequency ω. The polarization vector is oriented at an angle Θ_{o} with respect to the birefringent axis x' (Fig. 1) and is incident normally to the (1$\bar{1}$0) face. In the crystal the incident wave is split into two elliptic eigenwaves:

$$\begin{aligned} \boldsymbol{L} &= L_{\mathrm{o}} (\boldsymbol{x}' - \mathrm{i} K \boldsymbol{z}') \mathrm{e}^{\mathrm{i}(\boldsymbol{k}_{\mathrm{L}} \cdot \boldsymbol{r} - \omega t + \delta_1)} , \\ \boldsymbol{R} &= R_{\mathrm{o}} (-\mathrm{i} K \boldsymbol{x}' + \boldsymbol{z}') \mathrm{e}^{\mathrm{i}(\boldsymbol{k}_{\mathrm{R}} \cdot \boldsymbol{r} - \omega t + \delta_2)} , \end{aligned} \tag{8}$$

where $\boldsymbol{L}$ and $\boldsymbol{R}$ are left-handed and right-handed elliptic eigenwaves, and $\boldsymbol{k}_{\mathrm{L}}$ and $\boldsymbol{k}_{\mathrm{R}}$ are the corresponding wave vectors. The amplitudes L_{o} and R_{o} and the phase angles δ_1 and δ_2 are related to A_{o}, Θ_{o}, and K [15, 16].

At the exit face of the crystal the two elliptic waves have acquired an additional phase difference. If we use an analyzer $\boldsymbol{P}$ after the crystal oriented at an angle Θ to the x axis we get

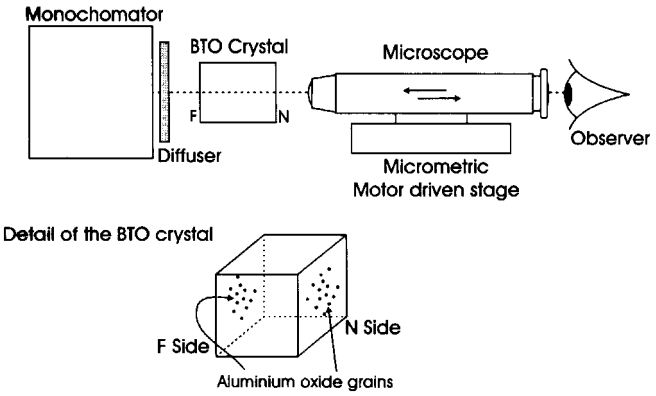

Fig. 2. Schematic diagram of the experimental setup for the measurement of the refractive index n of BTO

for the output light intensity after the analyzer

$$\begin{aligned} I &= [(\boldsymbol{L}+\boldsymbol{R})\cdot\boldsymbol{P}]\left[(\boldsymbol{L}+\boldsymbol{R})^*\cdot\boldsymbol{P}^*\right] \\ &= \left[L_\mathrm{o}^2+K^2R_\mathrm{o}^2-2KL_\mathrm{o}R_\mathrm{o}\sin(\phi l+\delta_0)\right]\cos^2\Theta \\ &+ \left[K^2L_\mathrm{o}^2+R_\mathrm{o}^2+2KL_\mathrm{o}R_\mathrm{o}\sin(\phi l+\delta_0)\right]\sin^2\Theta \\ &+ 2L_\mathrm{o}R_\mathrm{o}(1+K^2)\cos(\phi l+\delta_0)\cos\Theta\sin\Theta\,, \end{aligned} \tag{9}$$

$$\phi = k_\mathrm{L}-k_\mathrm{R} = \frac{2\pi}{\lambda_\mathrm{o}}(n_\mathrm{L}-n_\mathrm{R}), \qquad \delta_0 = \delta_1-\delta_2\,,$$

where k_L and k_R are the wavenumbers and n_L and n_R are the refractive indices of the eigenwaves.

This equation is further simplified if we consider the special case $\Theta_\mathrm{o}=45°$ (90° to the x axis) since for this case L_o, R_o and δ_0 are given by

$$L_\mathrm{o} = R_\mathrm{o} = \frac{1}{\sqrt{2}}\frac{A_\mathrm{o}}{\sqrt{1+K^2}}\,, \qquad \delta_0 = 0\,. \tag{10}$$

Consequently for $\Theta_\mathrm{o}=45°$, (9) becomes

$$I = \left[\frac{1}{2}+\Delta\cos(2\Theta-\psi)\right]A_\mathrm{o}^2\,, \tag{11}$$

where

$$\begin{aligned} \Delta &= \sqrt{\left(\frac{K}{1+K^2}\right)^2\sin^2(\phi l)+\frac{1}{4}\cos^2(\phi l)}, \\ \cos\psi &= -\frac{1}{\Delta}\frac{K}{1+K^2}\sin(\phi l)\,, \\ \sin\psi &= \frac{\cos(\phi l)}{2\Delta}. \end{aligned} \tag{12}$$

According to (11), the light intensity after the analyzer varies between $(\frac{1}{2}+\Delta)A_\mathrm{o}^2$ and $(\frac{1}{2}-\Delta)A_\mathrm{o}^2$ for rotation of the analyzer. Obviously for $\Delta=\frac{1}{2}$ the light is linearly polarized behind the crystal. This condition is fulfilled for $K=1$ or $\phi l=\pi, 2\pi, \ldots$. Then (5), (6) and (7) yield

$$r_\mathrm{eff} = \left(\frac{2\pi}{\lambda}n^3E_0\right)^{-1}\sqrt{\left(\frac{m\pi}{l}\right)-(2\varrho_0)^2}\,, \qquad m=1,2,\ldots. \tag{13}$$

We note from (13) that by measuring the voltage at which the ellipticity becomes zero, and knowing ϱ_0, we can determine the effective electro-optic coefficient r_eff [17]. The polarization angle of the linearly polarized wave will be 0° to the $\langle 110\rangle$ axis for $m=1,3,\ldots$ and 90° to the $\langle 110\rangle$ axis for $m=2,4,\ldots$ as can be easily derived from (11).

2 Experimental methods and results

In all our measurements we use an undoped BTO crystal with dimensions 8 mm × 8 mm × 8 mm.

2.1 Measurement of the index of refraction $n(\lambda)$

The experimental setup is shown in Fig. 2 and consists mainly of a microscope mounted on a step motor stage that is capable of motion of a few centimetres with a step width of 0.1 μm. The crystal is mounted in an adjustable holder and placed in the exit slit of a single-prism monochromator in front of a horizontal microscope. The bandwith of the light is about 6 nm. A diffuser placed between the monochomator exit slit and the crystal reduces the microscope's depth of focus to about 1 μm.

The distance between the sides F (far side of the crystal) and N (near), perpendicular to the microscope's optical axis, is measured with a micrometer stage, which is used for line spectra measurements, and is capable of measuring up to 1 μm: (FN) $= l = 7.908 \pm 0.005$ mm. In order to focus on the crystal surfaces we scattered a few grains of aluminium oxide (0.5 μm) on them. The microscope is first focused on a grain at F, and its position is read, then on a grain at N, and the new position is measured. Since the angles of incidence of the rays entering the microscope are very small, to a high degree of approximation the distance the microscope is moved between readings is equal to the actual distance FN divided by the index of refraction of the crystal [18]. The measurements are repeated six times for each wavelength and a mean value is taken. The index of refraction $n(\lambda)$ is determined with an absolute accuracy of ± 0.003 by using this method.

In Fig. 3 we plot the index of refraction n as a function of the wavelength λ. The theoretical curve is a least-squares fit of (1) to the experimental points. The obtained parameters are $\lambda_0 = 233$ nm and $S_0 = 8.99\times10^{-5}\,\mathrm{nm}^{-2}$. Morrison [19] measured a refractive index of $n = 2.55\pm0.035$ at $\lambda = 633$ nm, which coincides well with our result of $n = 2.578$. Our results are also in excellent agreement with the data published by Mersh et al. [20] ($\lambda_0 = 227$ nm and $S_0 = 9.40\times10^{-5}\,\mathrm{nm}^{-2}$).

2.2 Measurement of the rotatory power $\varrho_0(\lambda)$

The crystal is placed between a polarizer and an analyzer and is illuminated by a collimated monochromatic beam, which is obtained from a halogen lamp and a single-prism monochromator. The bandwidth of the light is about 6 nm. A photomultiplier is used as a detector. We measure the angle of rotation of the polarization plane by rotating the analyzer until extinction. The obtained angle of rotation divided by the crystal's thickness yields the rotatory power ϱ_0.

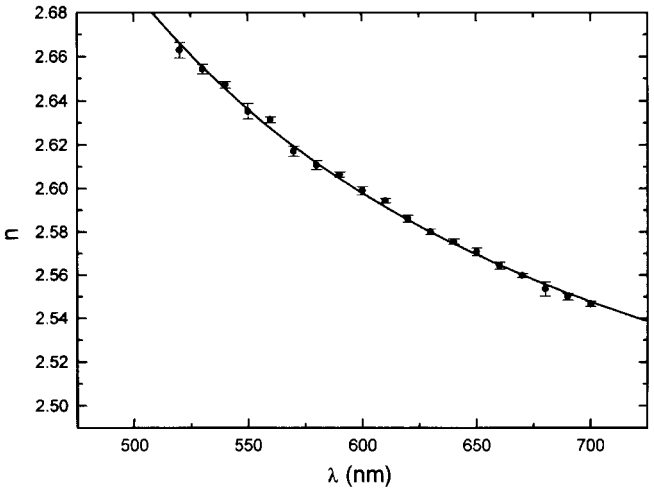

Fig. 3. Experimental results (*dots*) for the refractive index n of BTO and a fitted theoretical curve (*solid line*) based on the single-term Sellmeier equation versus the light wavelength λ. The error bars represent the standard deviation of each measurement set

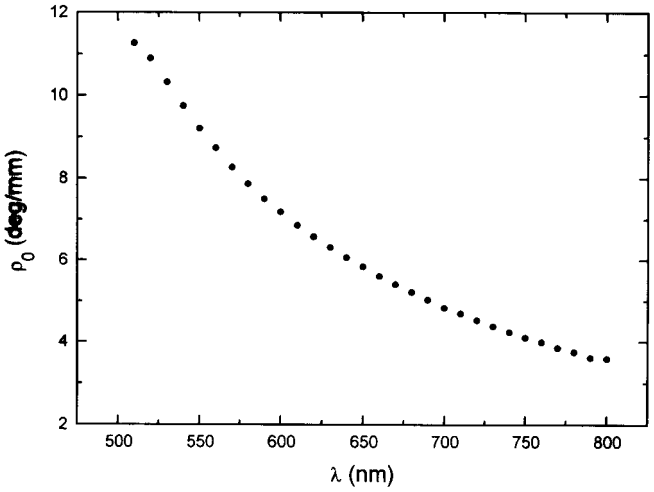

Fig. 4. Optical rotatory power ϱ_0 of the BTO crystal as a function of the light wavelength λ

In Fig. 4 we plot the results as a function of the wavelength λ. Our results are in excellent agreement with the data published by Mersh et al. [20] and in fairly good agreement with the data published by Feldman et al. [7] and McCahon et al. [8]. BTO exhibits very low optical activity compared with other similar materials such as BGO and BSO [7, 10].

2.3 Measurement of the electro-optic coefficient r_{41}

Our method consists of determining the zero ellipticity voltage for a specific polarization of the incident light beam ($\Theta_0 = 45°$ which is 90° to the ⟨110⟩ axis). A schematic diagram of the experimental setup is shown in Fig. 5. A collimated beam of monochromatic light, obtained from a Hg-Xe high-pressure white-light lamp passes through an interference filter and illuminates the BTO crystal. P_1 and P_2 are linear polarizers mounted on rotatory stages with angular scales. First, for a fixed position of P_1 (90° to ⟨110⟩) the ellipticity of the output beam is measured for various ap-

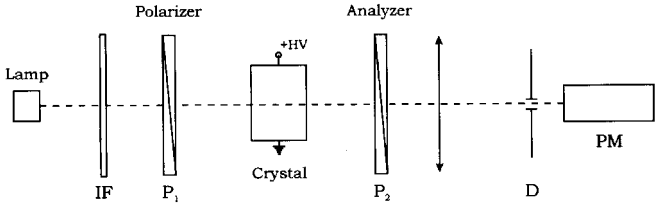

Fig. 5. Schematic diagram of the experimental setup for the measurement of the electro-optic coefficient. IF interference filter; HV high voltage; D hole; PM photomultiplier

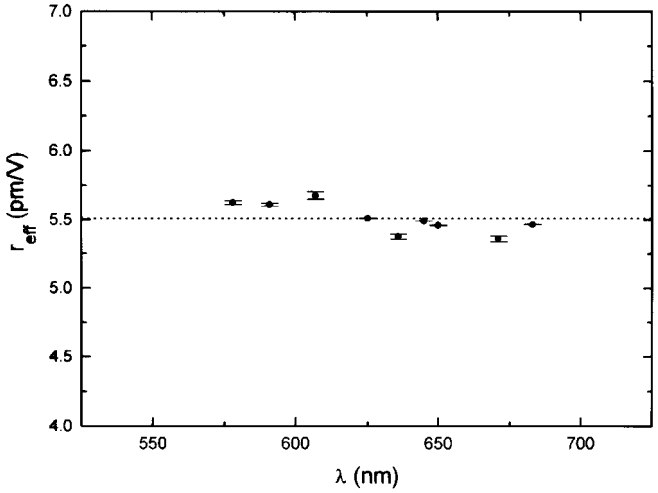

Fig. 6. Experimental results (*dots*) for the effective electro-optic coefficient r_{eff} of BTO versus wavelength λ. The error bars represent the standard deviation of each measurement set. The *dotted line* represents the mean value of all measured r_{eff} values

plied voltages. This gives us a rough estimate of the zero-ellipticity voltages. Then P_2 is set to 0° (or 90° to ⟨110⟩) and the applied high voltage, V, is fine tuned until a minimum output intensity is reached. Since $E_0 = V/d$ (d is the width of the crystal) r_{eff} can be calculated by (13). The material parameters, $n(\lambda)$ (Fig. 3), $\varrho_0(\lambda)$ (Fig. 4), $l = 7.908\,\text{mm}$, and $d = 8.0\,\text{mm}$ are used for the calculations. In our experiments, the process is repeated for various wavelengths.

Owing to the photoconductive property of the BTO crystals, screening charges build up because of nonuniformity in the illumination or because of blocking contacts [21, 22] the outcome being that the internal field may vary from the assumed value of V/d. The effect is stronger as the externally applied field is increased [9, 17]. The screening-charge build-up can be prevented if a sufficiently-high-frequency square-wave high voltage is applied externally to the crystal [23]. Because of its low optical activity, BTO exhibits two ellipticity minima in the 0 to 10 kV/cm range for wavelengths ranging from 500 nm to 700 nm. Therefore, to minimize the influence of the screening charges we use only the first ellipticity minimum in our calculations.

In Fig. 6 we plot r_{eff} as a function of the wavelength. The error bars represent the standard deviations. Within the experimental error the effective electro-optic coefficient has no measurable dispersion in the 578–683 nm wavelength range. The calculated mean value of r_{eff} plotted as a hori-

zontal dotted line in Fig. 6, was found to be $5.5 \pm 0.1\,\mathrm{pm/V}$ where the ± 0.1 error represents the standard deviation. If we subtract the piezoelectric contribution ($0.21\,\mathrm{pm/V}$ [14]) we get a value of $r_{41} = 5.3 \pm 0.1\,\mathrm{pm/V}$ which is in satisfactory agreement with the results in [24], where $r_{41} = 5.17\,\mathrm{pm/V}$ is obtained.

3 Concluding remarks

In this paper we present experimental data for the index of refraction and the optical activity of BTO crystals. In order to find a convenient and accurate technique for the measurement of the effective electro-optic coefficient, we study the electric field-induced birefringent properties of electro-optic BTO crystals for the transverse configuration. The electrogyration and the so-called secondary electro-optic effect (inverse piezoelectric and photoelastic effects) are taken into account. Analytic expressions are derived for the ellipticity of the polarization of a light beam passing trough a BTO crystal as a function of the crystal properties and of the orientation of the incident light vector.

We apply these expressions to the special case of light with an incident polarization parallel to the $\langle 001 \rangle$ axis, which is symmetrically oriented to the birefringence axes x' and z'. From the simplified expressions we deduce the interesting result that after passing trough the crystal the light is linearly polarized for a specific set of values of the induced birefringence and thus of the applied electric field. The output polarization is either normal or parallel to the incident-light polarization. A simple relation is derived, yielding the effective electro-optic coefficient r_{eff} from the above-mentioned externally applied electric field. The demonstrated method is precise and very simple to operate.

References

1. J.P. Herriau, J.P. Huingnard, A.G. Apostolidis, S. Mallick: Optics Commun. **56**, 141 (1985)
2. M.P. Petrov, S.V. Miridonov, S.I. Stepanov, V.V. Kulikov: Optics Commun. **31**, 301 (1979)
3. D. Tontchev, S. Zhivkova, M. Miteva: Appl. Opt. **29**, 4753 (1990)
4. R.E. Aldrich, S.L. Hon, M.L. Harwill: J. Appl. Phys. **42**, 493 (1971)
5. Fr. Vachss, L. Hesselink: Optics Commun. **62**, 159 (1987)
6. P. Pellat-Finnet: Optics Commun. **50**, 275 (1984)
7. A. Feldman, W.S. Brower Jr., D. Horowitz: Appl. Phys. Lett. **16**, 201 (1970)
8. S.W. McCahon, D. Rytz, G.C. Valley, M.B. Klein, B.A. Wechsler: Appl. Opt. **28**, 1967 (1989)
9. M. Henry, S. Mallick, D. Rouède, L.E. Celaya, A. Garcia Weidner: J. Appl. Phys. **59**, 2650 (1986)
10. P.V. Lenzo, E.G. Spencer, A.A. Baliman: Appl. Opt. **5**, 1688 (1966)
11. M. DiDomenico Jr., S.H. Wemple: J. Appl. Phys. **40**, 720 (1969)
12. J.F. Nye: *Physical Properties of Crystals* (Clarendon Press, Oxford 1957)
13. T.A. Maldonado, T.K. Gaylord: Appl. Opt. **28**, 2075 (1989)
14. S.I. Stepanov, S.M. Shandarov, N.D. Khatkov: Sov. Phys. Solid State **29**, 1754 (1987)
15. S. Mallick, D. Rouède, A.G. Apostolidis: J. Opt. Soc. Am. B **4**, 1247 (1987)
16. A.G. Apostolidis, S. Mallick, D. Rouède, J.P. Herriau, J.P. Huignard: Optics Commun. **5**, 73 (1985)
17. D.G. Papazoglou, A.G. Apostolidis, E.D. Vanidhis: **G-IV**/**P17** E-MRS 1996 Spring Meeting Strasbourg (France) June 4–7 1996 (To be published in Synthetic Metals)
18. G.S. Monk: *Light Principles and Experiments* (Dover, New York 1963)
19. A.D. Morrison: Ferroelectrics **2**, 59 (1971)
20. F. Mersch, K. Buse, W. Sauf, H. Hesse, E. Krätzig: Phys. Stat. Sol. (a) **140**, 273 (1993)
21. V.V. Bryksin, L.I. Korovin, Yu.I. Kuz'min: Sov. Phys. Solid State **29**, 757 (1987)
22. V.N. Astratov, A.V. Il'inskii, V.A. Kiselev: Sov. Phys. Solid State **26**, 1720 (1984)
23. A. Grunnet-Jepsen, I. Aubrecht, L. Solymar: J. Opt. Soc. Am. B **12**, 921 (1995)
24. A.J. Fox, T.M. Bruton: Appl. Phys. Lett. **27**, 360 (1975)